Transmission Electron Spin Resonance in Dilute Copper-Chromium Alloys*

P. MONOD† AND S. SCHULTZ
Department of Physics, University of California, San Diego, La Jolla, California 92038
(Received 8 April 1968)

Utilizing the transmission conduction-electron spin-resonance technique, we have observed the spin resonance associated with the combined local-moment–conduction-electron system in Cu-Cr over the temperature range 1.4–40°K and concentration range 4–36 ppm. The measured g values, linewidths, and lineshape parameters are interpreted utilizing the Hasegawa model extended to include electron magnetization diffusion and additional local-moment relaxation modes. The predictions of this phenomenological model successfully account for the behavior of the system and we are able to deduce the following parameters: the intrinsic g value for Cr in Cu (2.006 ± 0.002), the spin-flip scattering rate of the conduction electrons in copper by the Cr impurities ($1/T_{sl}=4.8\times10^{+7}$ sec^{-1}/ppm), the intrinsic (phenomenological) relaxation rate of the Cr to the copper lattice ($1/T_{dl}=2.1\times10^{9}$ sec^{-1}), a lower limit to the effective s-d exchange coupling ($|J|\geq0.3$ eV), and the ratio of the local moment to conduction-electron spin susceptibilities. Combining this ratio with a separate measurement of the local-moment susceptibility, we are able to determine the conduction-electron spin susceptibility of pure copper. This value, $(1.08\pm0.1)\times10^{-7}$ emu/g, is compared with the free-electron theory from which F_0, the first spin-dependent parameter of the Landau-Fermi liquid theory, is deduced.

INTRODUCTION

THERE have been numerous theoretical and experimental investigations into the effects of a "local moment" in a metallic host. Most of these investigations are interpreted within the framework of a simplifying initial assumption, that the system is described by a simple exchange interaction of the type $J\mathbf{S}_s\cdot\mathbf{S}_d$, where $\mathbf{S}_s$ and $\mathbf{S}_d$ represent a conduction-electron and local-moment spin, respectively. Experimental approaches to this problem have included resistivity,[1] magnetoresistance,[2] susceptibility,[3] specific heats,[4] Mössbauer effect,[5] oriented γ spectroscopy,[6] nuclear magnetic resonance (NMR),[7] and electron paramagnetic resonance (EPR).[8] While it is true that many principal features of the local-moment system are explained in terms of the simple exchange interaction, it has become increasingly clear that the problem is really a complex one and that finer or more microscopic probes of the spin system are needed to help point the way for further theoretical development. We report here the application of a relatively new approach to the local moment problem, namely, transmission electron spin resonance (TESR), which, being directly sensitive to various dynamic spin parameters such as g value and relaxation rates, offers the possibility of more exacting demands on theoretical models to account for the observed effects. EPR of local moments in metals by the reflection technique has been extensively used with Mn and Gd.[8] The scarcity of application of this technique to transition-metal impurities is simply due to the fact that Mn in noble metals represents the only case where confirmed paramagnetic resonance signals have been observed.[8,9] Recently, the application of the TESR technique has been reported by Cowan for *Cu*-Mn.[10] More detailed measurements, and a comparison with a phenomenological theory, has been presented by Schultz, Shanabarger, and Platzman,[11] who reported resonances in both *Cu*-Mn and *Ag*-Mn, as well as a presentation of certain striking properties of the coupled local-moment–conduction-electron spin system. In this paper we report the first observation of

* Work supported by the National Science Foundation.
† On leave from Laboratoire de Physique des Solides, Associé C. N. R. S., Faculté des Sciences, Orsay 91, France. Work supported by a North Atlantic Treaty Organization Fellowship, registered under No. A.O. 1783, at the Centre de Documentation du Centre National de la Recherche Scientifique, France.

[1] For a review of experimental work before Kondo's calculation, see *Progress in Low Temperature Physics*, edited by C. G. Gorter (North-Holland Publishing Co., Amsterdam, 1964), Vol. IV, p. 194. A more recent survey is made by M. D. Daybell and W. A. Steyert, Rev. Mod. Phys. (to be published).

[2] See Ref. 1 and P. Monod, Phys. Rev. Letters **19**, 1113 (1967); F. T. Hedgcock, W. B. Muir, T. W. Raudorf, and R. Szmidt, *ibid.* **20**, 457 (1968); M. D. Daybell and W. A. Steyert, *ibid.* **20**, 195 (1968).

[3] See Ref. 1 and J. A. Careaga, B. Dreyfus, R. Tournier, and L. Weil, in *Proceedings of the Tenth International Conference on Low Temperature Physics, Moscow, 1966* (Proizvodstrenno-Izdatel'skii Kombinat, VINITI, Moscow, 1967); M. D. Daybell and W. A. Steyert, Phys. Rev. Letters **18**, 398 (1967); C. M. Hurd, J. Phys. Chem. Solids **28**, 1345 (1967).

[4] See Ref. 1.

[5] R. B. Frankel, N. A. Blum, B. B. Schwartz, and D. J. Kim, Phys. Rev. Letters **18**, 1051 (1967).

[6] I. A. Campbell, J. P. Compton, I. R. Williams, and G. V. H. Wilson, Phys. Rev. Letters **19**, 1319 (1967).

[7] L. B. Welsh, A. J. Heeger, and M. A. Jensen, J. Appl. Phys. **39**, 696 (1968); M. A. Jensen, A. J. Heeger, L. B. Welsh, and G. Gladstone, Phys. Rev. Letters **18**, 997 (1967); L. B. Welsh, G. Gladstone, A. J. Heeger, and M. A. Jensen, Bull. Am. Phys. Soc. **13**, 410 (1968).

[8] J. Owen, M. Brown, W. D. Knight, and C. Kittel, Phys. Rev. **102**, 1501 (1956); A. C. Gossard, A. J. Heeger, and J. H. Wernick, J. Appl. Phys. **38**, 1251 (1967); M. Peter, J. Dupraz, and H. Coffet, Helv. Phys. Acta **40**, 316 (1967), and references therein.

[9] There are often references in the literature to "observations" of resonances attributed to both pure metals and added impurities. Much of this work has been spurious, and hence we restrict our designation of "confirmed" resonances to the cases mentioned.

[10] D. L. Cowan, Phys. Rev. Letters **18**, 770 (1967).

[11] S. Schultz, M. R. Shanabarger, and P. M. Platzman, Phys. Rev. Letters **19**, 749 (1967).

the resonance of Cr in Cu, utilizing the TESR technique. This is the first observation of spin resonance for a transition-metal impurity other than Mn in a metal.

The paper is organized as follows. Section I is a basic discussion of the TESR technique applied to a pure metal and an explanation of the signal actually measured; the principal effects on the TESR signal due to the addition of magnetic impurities are qualitatively discussed. Section II contains a brief description of the experimental equipment and the sample preparation. Section III presents the phenomenological theory of Hasegawa[12] as extended by Ref. 11, concluding with the formulas that are directly used to interpret the data. Section IV is a presentation of the data and their analysis utilizing the theory of Sec. III. Section V is a discussion of the results.

I. TESR TECHNIQUE

A. Pure Metals

In the usual (reflection) EPR experiments the metal sample is placed in a uniform dc magnetic field H_0 and an additional rf magnetic field H_1 is applied which is perpendicular to the dc field. When this applied rf frequency ω is close to the Larmor precession frequency of the spins, the sample absorbs power. The (generally small) power absorption is then detected by appropriate electronic equipment, and an analysis of the characteristic resonance observed yields the location of the resonant frequency (g value), relaxation rates (via linewidths), and other features depending on the line-shape analysis. The TESR technique differs in the way the response of the spin system to the excitation is observed.[13]

Since the observed resonance signals for local moments in metals are intimately connected with conduction electron spin resonance (CESR) in the pure metal, and since the final theoretical formulas we will utilize can be interpreted in terms of simple modifications of formulas for the pure CESR, it is worth while to first discuss this case. Consider the sample to be a thin infinite sheet of a metal with the rf magnetic field incident on one side (transmit) and a sensitive detector on the other (receive) side (Fig. 2). The transmitted field is strongly attenuated via the shielding effects of the conduction electrons. In practice the sample is a sufficient number of skin depths thick that this transmitted source of power is negligible. The TESR technique makes use of the fact that when one is near the resonant frequency, electrons within a skin depth of the transmit surface respond to the excitation field and develop a net transverse magnetization. Then, via a diffusion process they carry this information (i.e., a nonequilibrium magnetization) deep into the metal and over to the far side.[14] At the far side, one simply has a precessing transverse magnetization which radiates power. Thus, if, as usual, one sweeps the dc magnetic field while applying a fixed frequency rf field, one expects zero transmitted power except in the vicinity of the resonant field.[15] In addition to the usual requirement that the relaxation time of the transverse magnetization, T_2, not be too short (so that the resonance line is observable), one has the additional physical requirement that the characteristic diffusion length (δ_s) of the electronic magnetization in the relaxation time T_2 be equal to or greater than the thickness of the sample. For a simple three-dimensional random walk, $\delta_s^2=\frac{2}{3}v_F^2\tau T_2$, where v_F is the Fermi velocity and τ is the momentum collision time. In practice the requirement of a long T_2 and a long τ usually requires pure samples and sufficiently low temperatures such that the phonon contribution to both relaxation times is negligible.

Although the radiated power may be directly detected, it is often advantageous to be able to detect the in-phase and out-of-phase components of the transmitted field relative to the incident field. This is accomplished by detecting the transmitted field in the presence of a larger reference field at the same frequency whose phase can be arbitrarily changed. The component of the transmitted field projected along the reference field is called the signal. As one sweeps through a resonance, there is an increasing magnitude of the transmitted field accompanied by a continuous phase shifting. Consequently, depending on the nature of the signal and its phase relationship to the reference, it is possible to generate "signals" which can be both positive and negative with respect to the baseline. A typical signal and the characteristics that we measure are shown in Fig. 1. All data for this paper were taken with the reference phase adjusted so that the side lobe amplitude were equal, i.e., $B=B'$. In general, this does not necessarily mean that $\alpha=\alpha'$; the significance of such asymmetry is discussed in Sec. IV. (See insert in Fig. 5.)

The general solution of the transmission problem for the case of CESR has been given by Lampe and Platzman,[16] who extended Dyson's work[17] for the reflection case. Under normal skin effect conditions, it is

[12] H. Hasegawa, Progr. Theoret. Phys. (Kyoto) **21**, 483 (1959).

[13] A detailed analysis of the TESR technique will be presented in other publications and in G. L. Dunifer, thesis, University of California, San Diego (unpublished).

[14] In practice, for pure metals, other efficient modes of microwave power transmission are possible. This generally gives rise to a large and complicated "background" pattern of signals (a complete discussion of these modes is in preparation). However, they exist only if $\omega_c\tau>1$, where ω_c is the cyclotron frequency. In our alloys this condition is not met and the TESR signal appears alone on a flat base line.

[15] It should be emphasized that the ability to detect only the power that has been transmitted *through* the sample serves to effectively discriminate against spurious resonances due to paramagnetic impurities in the cavities, etc. This is to be contrasted to the usual reflection technique, where changes in absorbed power in the cavity due to all causes are superimposed.

[16] M. Lampe and P. M. Platzman, Phys. Rev. **150**, 340 (1966).

[17] F. J. Dyson, Phys. Rev. **98**, 349 (1954).

particularly simple to solve Maxwell's equations combined with a Bloch equation for the spins modified to include a diffusion term $D\nabla^2\mathbf{M}$. The solution in the case for the dc field perpendicular to the sample has been given by Vander Ven and Schumacher,[18] and an alternative but equivalent approach has been taken by Lewis and Carver.[19] Extensive calculations of line shapes, etc., have been compiled by Dunifer.[13] The main conclusions are the following: The essential parameters which characterize a symmetrized signal as in Fig. 1 are the g value, T_2, and the ratio $\Delta_s=\delta_s/L$, where L is the sample thickness. The value of Δ_s is uniquely determined by the measured peak height A to lobe B ratio (see Fig. 1). Once Δ_s is known, T_2 is recovered from the linewidth ΔH using the relation $\gamma T_2\Delta H=k$, where γ is the electron gyroscopic ratio, and k is a parameter which is determined from computer solutions to the problem for given values of Δ_s.[13] In the limit in which Δ_s gets large (long diffusion lengths, thin samples) the A/B ratio gets very large, the line shape approaches a Lorentzian, and $k=2$.

B. Metals Containing Magnetic Impurities

The brief physical picture just given adequately describes the behavior of CESR in pure metals.[17,20] If we now include the presence of randomly distributed dilute local moments, we can expect several major effects. In this section we shall just indicate their nature in a qualitative way and discuss them in detail in Secs. III and IV.

The effects of the magnetic impurities on the spin-resonance signal are complex[12,21] and will not be discussed in the general case. We restrict ourselves to the special situation where (a) the g factor of the impurity, g_d, is very close to that of the conduction electrons (g_s), and (b) the mutual spin-flip rate between the two spin systems is larger than any relaxation rates to the lattice. These conditions are easily satisfied in the *Cu*-Cr system. A consequence of these conditions is that both magnetizations are collinear and in equilibrium with each other at all times. On the other hand, the resultant magnetization is not necessarily in equilibrium with the lattice. The relaxation mechanisms of each spin system will contribute to an over-all relaxation rate $1/T_{\text{eff}}$. The dominant response of this strongly coupled system to an rf exciting field will appear as a single resonance line.[22] However, the behavior of this

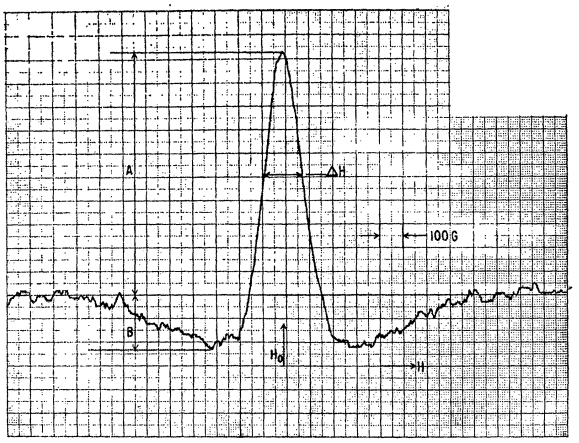

FIG. 1. Transmission spin resonance signal of a 35 at. ppm *Cu*-Cr sample (25 μ thick) at 24.5°K and 3200 G. The use of the measured resonant field H_0, linewidth ΔH, and line-shape factor A/B to analyze the properties of the spin system is discussed in the text.

resonance is analyzed in terms of the parameters of each spin system.

The most important parameter is the quantity $\chi_d/\chi_s=\chi_r$, that is, the ratio of the impurity static susceptibility to that of the conduction electron susceptibility. Whenever χ_r is much smaller than 1, the properties of the conduction electron system will dominate and the resonance signal will behave essentially like the pure metal resonance. On the other hand, when χ_r becomes larger than 1 (at low temperatures or higher concentration of magnetic impurities), the resonance will be dominated by the intrinsic properties of the local moments. In our experiments, χ_r is varied over the range 0.01–10.[23]

All the parameters of the TESR signal such as the amplitude, linewidth, g value, magnetization diffusion constant, and the symmetry of the line depend on χ_r. Consequently, as the temperature is varied, these will change. For example, at sufficiently low temperatures the g value of the line will be close to the intrinsic g value of the magnetic impurity g_d, and will shift, as one warms up the sample, approaching the value appropriate to the host metal (g_s).

We pointed out that in a pure metal the TESR line shape is characterized by three parameters: g_s, T_2, and Δ_s. In our present case, the TESR line shape is characterized by three analogous quantities g_{eff}, T_{eff}, and Δ_{eff}, which are all functions of χ_r. Furthermore, the relations describing the signal in terms of these analogous quantities are identical to those for the case of the pure metal. This formal identification enables

[18] N. S. Vander Ven and R. T. Schumacher, Phys. Rev. Letters **12**, 695 (1964).
[19] R. B. Lewis and T. R. Carver, Phys. Rev. **155**, 309 (1967).
[20] S. Schultz and M. R. Shanabarger, Phys. Rev. Letters **16**, 178 (1966); S. Schultz and C. Latham, *ibid.* **15**, 148 (1965); S. Schultz, G. L. Dunifer, and C. Latham, Phys. Letters **23**, 192 (1966).
[21] C. R. Burr and R. Orbach, Phys. Rev. Letters **19**, 1133 (1967); D. Griffiths and B. R. Coles, *ibid.* **16**, 1093 (1966).
[22] The equations of motion always possess two possible modes. In our case, however, the other solution is strongly damped by the cross relaxation rate $1/T_{ds}$ and would correspond to the motion of one magnetization with respect to the other.
[23] Peter *et al.* (Ref. 8) refer to many alloys of magnetic impurities at concentration of the order of 1%, and hence the experiments are always done under the condition of $\chi_r\gg1$. One would then expect that the information available from the ESR signal only pertains to the intrinsic properties of the impurity. In particular, we believe that this may account for the striking similarity of reported resonances for Mn dissolved in various hosts.

us to easily determine these quantities from the observed line shapes utilizing the same procedures outlined for the case of the pure metal.

II. EXPERIMENTAL

A. TESR Apparatus

A block diagram showing the essential features of a TESR spectrometer system is shown in Fig. 2. Additional supplementary equipment is needed to make cavity Q measurements, frequency determination, power levels, etc. The power oscillator is an X-band ultrastable klystron supply with a power output of approximately 250 mW over the range 8.6–10.0 kMHz. Part of the cw output is taken off via a 20-dB coupler to serve as the reference while the main power passes through a diode modulator operated at an audio frequency (typically 1000 Hz). Sufficient isolation is placed in the line to insure that a negligible amount of modulated power is reflected back to the reference arm. A TE 101 cavity with a variable coupler is used on each side of the sample to improve the impedance match between the spin system and the microwave components. The modulated microwave field that is transmitted through the sample via the spins is combined with the reference field and detected in a superheterodyne receiver which has a limiting sensitivity of $\sim 10^{-20}$ W (1-sec time constant).

The receiver consists of a balanced mixer followed by a 60 Mc/sec i.f. strip. The audio signal is detected utilizing a phase-sensitive amplifier whose reference signal is the timing source for the modulation of the diode switch. The output is displayed on a twin track or X-Y recorder along with such field information as is necessary.

In order to exploit the full sensitivity of the transmission method it is essential that any spurious leakage of microwave power around the sample be as small as possible. In addition, the reliability that the field variation of the modulated microwave field is due to transmission through the sample is increased as the leakage power (which is also modulated) is reduced. For a maximum power input of approximately 100 mW and a detection level of 10^{-19} W this implies a microwave isolation between cavities of the order of 180 dB.[13]

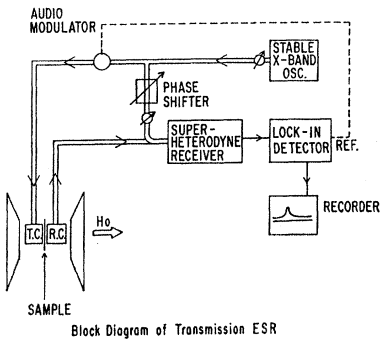

FIG. 2. Block diagram of the TESR spectrometer.

The temperature of the cavities (in intimate contact with the sample) is measured using calibrated carbon or platinum resistors in their appropriate ranges. The accuracy is everywhere better than ± 0.1°K. The temperature is set by having the cavities thermally connected to a liquid helium bath and adjusting the power in a heater resistor with an appropriate electronic control system. A standard set of glass helium and nitrogen Dewars are used to obtain the cryogenic temperatures.

The dc magnetic field is regulated and programmed utilizing the Varian FielDial and 12-in. magnet system. The magnet may be rotated. Although field modulation is normally not used in the TESR method, it is utilized when the system is operated as a reflection spectrometer. This is done to calibrate the actual field at the surface of the sample by looking at the resonance of a small piece of neutron-irradiated LiF so placed. The g value of the signal from the Li particles in the sample is taken as 2.0023.[24] In addition, NMR markers are utilized to calibrate the field sweeps to determine linewidths.

B. Susceptibility

The static susceptibility of the 36-ppm ingot was measured utilizing a Faraday balance susceptibility apparatus.[25] The measured susceptibility of the local moments over the temperature range 1.4–25°K obeys the relation $\chi_d = N(P_{\text{eff}})^2/3k(T+T')$, where N is the number of Cr impurities and k is the Boltzmann constant. We find $P_{\text{eff}}{}^2 = 15.5 \pm 1$ (Bohr magnetons)^2 corresponding very nearly to a spin of $\frac{3}{2}$. T' is found to be 1 ± 0.5°K, which is very close to the "Kondo temperature" for this system inferred from resistivity and NMR data.[7,26] The precision of the susceptibility measurements was 10^{-9} emu, but the accuracy was somewhat less because of necessary sample holder corrections.

C. Sample Preparation and Analysis

Samples were prepared by successive dilutions of a master alloy with pure copper.[27] Single crystals were grown via the Bridgman technique in aluminacoated graphite crucibles. The ambient vacuum was $\sim 10^{-6}$ Torr and rf heating was utilized to insure adequate mixing with only a relatively short time at high temperatures. The samples for the TESR were spark-cut

[24] The resonance signal from the Li particles in the neutron-irradiated LiF was checked to be 2.0023 by comparison with transmission signals in pure Li.

[25] D. W. Wohlleben, thesis, University of California, San Diego (to be published); D. W. Wohlleben and G. S. Knapp, Rev. Sci. Instr. (to be published).

[26] See M. D. Daybell *et al.* (Ref. 3).

[27] P. Monod, thèse, Université d'Orsay, Orsay 91, France (to be published).

from the ingots and carefully chemically lapped and polished to a thickness of about 25 μ. Other pieces of the ingot were retained for resistivity, atomic optical-absorption analysis, neutron activation, and susceptibility measurements.

III. PHENOMENOLOGICAL MODEL

In this section we shall outline the derivation of the TESR signal equations based on a modified model of the *s-d* system originally described by Hasegawa.[12] These results were presented in Ref. 11, where the authors attempted to account for their observed data on the *Cu*-Mn system.

The essential features of Hasegawa's model are a strongly coupled local-moment–conduction-electron spin system interacting via an exchange interaction and a weaker coupling of the conduction electrons to the lattice. The mutual spin cross relaxation times are called T_{sd} and T_{ds}, respectively, and can be expressed in terms of J. See Fig. 3. This model predicts a "bottleneck effect" if the conduction electron relaxation to the lattice is sufficiently weak. The consequences of this have been exploited by Gossard *et al.*[8] to determine the effect of nonmagnetic impurities on T_{sl}. The modifications to this model proposed by Ref. 11 are: different g values for the electrons and local moments, a phenomenological direct relaxation path from the local moments to the lattice (T_{dl}), and the effects of electron diffusion.

We briefly review the basic equations for the magnetization, present the solutions for a thin slab as given in Ref. 11, and then focus on those relations which are used to interpret the data.

The equation of motion of each component of the total magnetization is written as[11,28]

$$\frac{d\mathbf{M}_s}{dt}=\gamma_s[\mathbf{M}_s\times(\mathbf{H}+\lambda\mathbf{M}_d)]-\frac{\chi_r\mathbf{M}_s-\mathbf{M}_d}{T_{ds}}-\frac{\mathbf{M}_s-\mathbf{M}_s^0}{T_{sl}}+D\nabla^2\mathbf{M}_s, \quad (1)$$

[28] The Larmor-precession term in the equation of motion of each magnetization is written as if the effect of the other magnetizations could be represented by a uniform molecular field. This is obviously an approximation because one knows that the magnetization of the impurities is highly localized. Furthermore, this picture would lead to an additional Knight shift (see Ref. 12) of the copper nuclei far removed from any magnetic impurity, which is not observed. The model can be used, however, because the rate of collision of the conduction electrons with the magnetic impurities is much greater than the Larmor frequency of the spins. Hence, the diffusing electron spins see an effective "molecular" field corresponding to an average over the spatial distribution of the impurity magnetization. The mathematical form of Eqs. (1) and (2) is only correct if $g_s=g_d$ and if one assumes that the relaxation of the magnetization occurs towards the equilibrium field rather than the instantaneous field. (See Refs. 12, 30, and 34.) When $g_s\neq g_d$, these equations and their solution become more complex. But in our case the simple form of Eqs. (1) and (2) is still valid to order g_s/g_d because $(g_d-g_s)/g_s\sim 1\%$. As pointed out to us, a new source of broadening appears, which is (see Ref. 30)

$$\Delta H(g_s-g_d)=\frac{(\gamma_s-\gamma_d)^2H_0^2}{1/T_{ds}+1/T_{sd}}\frac{\chi_0^s\chi_0^d}{(\chi_0^s+\chi_0^d)^2}.$$

This quantity is negligible in our case but may become important for rare-earth impurities. A detailed account of this question is being investigated (Ref. 30).

[29] The details of the calculation will appear in M. R. Shanabarger, thesis, University of California, San Diego (unpublished).

[30] Y. Yafet (private communication).

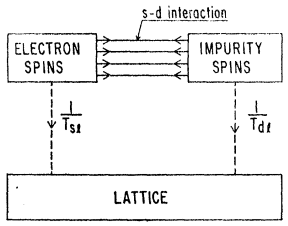

FIG. 3. A representation of the spin systems and relaxation paths used in developing Hasegawa's equations. The *s-d* interaction is the cross relaxation mechanism that brings the impurity spins and electron spins into equilibrium with each other.

$$\frac{d\mathbf{M}_d}{dt}=\gamma_d[\mathbf{M}_d\times(\mathbf{H}+\lambda\mathbf{M}_s)]+\frac{\chi_r\mathbf{M}_s-\mathbf{M}_d}{T_{ds}}-\frac{\mathbf{M}_d-\mathbf{M}_d^0}{T_{dl}}, \quad (2)$$

where $\gamma_{s(d)}=g_{s(d)}\mu_B/\hbar$ and λ characterizes the effective field coupling the two magnetizations; it is given in terms of the exchange integral J by

$$\lambda=2J\Omega/\gamma_s\gamma_d\hbar^2, \quad (3)$$

where Ω is the atomic volume. D is the diffusion constant of the conduction electrons; $D=\frac{1}{3}v_F^2\tau$, where τ is the momentum collision time. The relaxation time T_{ds} is given in terms of J by the Korringa relation

$$\frac{1}{T_{ds}}=\frac{4\pi}{\hbar}J^2\rho(\epsilon_F)^2kT, \quad (4)$$

where $\rho(\epsilon_F)$ is the density of state per atom for one spin direction, at the Fermi level. M_s^0 and M_d^0 are the equilibrium values of the magnetization of the s and d spin systems. From the structure of the equation of motion, it is evident that as long as M_s and M_d remain collinear there cannot be a large g shift of the observed system resonance (analogous to the Knight shift) nor can there be any width due to the cross relaxation mechanism.[28]

When, for sufficiently large J, the condition

$$|\omega_s-\omega_d|<|\lambda\chi_s\omega_s+i/T_{ds}| \quad (5)$$

is fulfilled, that is, the difference in Larmor frequency of the two systems is smaller than either the cross relaxation rate or the Larmor frequency in the "molecular" field, the transmitted field $H_t(\omega)$ through a sample of thickness L will be[11,22,29,30]

$$H_t(\omega)=(Q/K_2)(1+\chi_r)^2 1/\sinh(K_2L), \quad (6)$$

with

$$D_0K_2^2=(1/T_{\rm eff})[1+i(\omega-\omega_0)T_{\rm eff}] \quad (7)$$

and

$$D_0=\tfrac{1}{3}v_F^2\tau/(1+\chi_r)\,, \quad (8)$$

where Q is a constant.[29] Note that at resonance $K_2=1/\delta_{\rm eff}$.

For this solution the transmitted signal is symmetric around the resonance field.[13] The g value of the resonance, g_0, is given as a function of the g factor of electrons, g_s, and Cr impurities, g_d, by

$$g_s-g_0=(g_s-g_d)\chi_r/(1+\chi_r)\,. \quad (9)$$

$1/T_{\rm eff}$ is the effective relaxation rate of the combined system. It is given in terms of the relaxation rate of each system by

$$\frac{\chi_s+\chi_d}{T_{\rm eff}}=\frac{\chi_s}{T_{sl}}+\frac{\chi_d}{T_{dl}}\,. \quad (10)$$

It can be rewritten only involving χ_r as

$$\frac{1}{T_{\rm eff}}=\frac{1}{T_{sl}}\frac{1}{1+\chi_r}+\frac{1}{T_{dl}}\frac{\chi_r}{1+\chi_r}\,. \quad (11)$$

As was mentioned in Sec. II, the new quantities g_0, D_0, and $T_{\rm eff}$ enter into the signal formulas with the same relations as in the CESR problem.[13,19,20] It is of interest to note that the temperature and concentration dependence of these quantities happen mainly through χ_r. In particular, the effective diffusion coefficient of the total magnetization (which determines the line shape and its amplitude) will become smaller as the concentration increases, not only because of the shortening of the collision time τ, but also because of the presence of the additional magnetization of the local moments which cannot diffuse by itself, and slows down the diffusion of the electron magnetization.

Equations (8), (9), and (11) will be utilized in the comparison of theory and experiment.

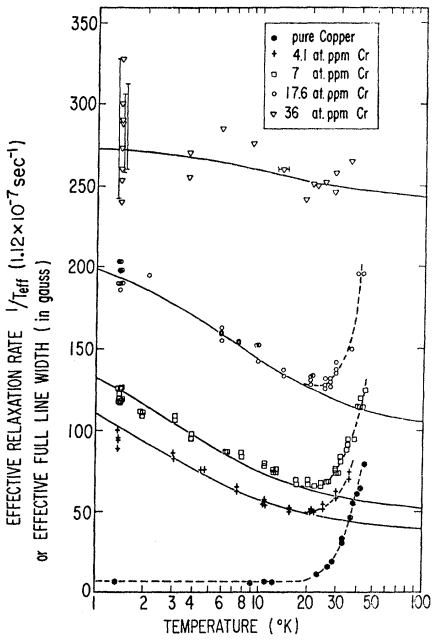

FIG. 4. Effective linewidth of the TESR signal versus temperature for different Cu-Cr samples and pure Cu. The striking *narrowing* of the resonance with increasing temperature agrees with the theoretical predictions of a modified Hasegawa model [Eq. (11); solid lines]. The calculations assume that the relaxation times are temperature-independent. This assumption breaks down above 20°K, where phonon spin scattering begins to contribute appreciably.

IV. EXPERIMENTAL RESULTS AND DATA ANALYSIS

Data were taken for seven samples ranging in concentration from 4 to 36 at. ppm at a frequency of $\simeq$9200 mHz. The linewidths and g values were measured as a function of temperature from 1.4°K to the highest temperatures at which meaningful signals could be observed, around 35°K. The linewidth data are converted to $1/T_{\rm eff}$ values (after measurement of the A/B ratios, when necessary) as described in Sec. II. The main features of the data are the following:

(1) *Linewidths.* All samples showed an appreciable (up to 50%) *narrowing* of the linewidth as the temperature is increased up to approximately 25°K. Above this temperature the linewidth broadens rapidly because of the increasing contribution of phonon scattering. The initial narrowing may appear intuitively somewhat surprising but has a relatively simple explanation. If one assumes that T_{sl} and T_{dl} are temperature-independent (before the phonons are important), then the temperature dependence in Eq. (11) is solely through χ_r. Hence, if $1/T_{dl}$ is large enough compared to $1/T_{sl}$, the second term will decrease fast enough with increasing temperature to yield a net narrowing of the line. Typical data for $1/T_{\rm eff}$ versus temperature are shown in Fig. 4.

(2) *Line shapes.* The data were always taken with the reference field adjusted so that the side lobes were equal ($B=B'$). Under this condition the line shapes were symmetric to within the experimental accuracy. As was mentioned in Sec. II, this allows one to set a lower limit on the magnitude of the exchange interaction and we find $|J|\geq0.3$ eV. This is the experimental justification for utilizing the large exchange coupling limit formulas for comparison with the data. The A/B ratio was also measured and typical data are plotted versus temperature in Fig. 5. Knowing $T_{\rm eff}$, the sample thickness χ_r, and τ (from resistivity data), one can compute the A/B ratio from the predicted expression for the transmitted field [Eq. (8)]. These results are indicated in Fig. 5 as the solid lines. It is interesting to note that in this case of Cr in Cu we find very good

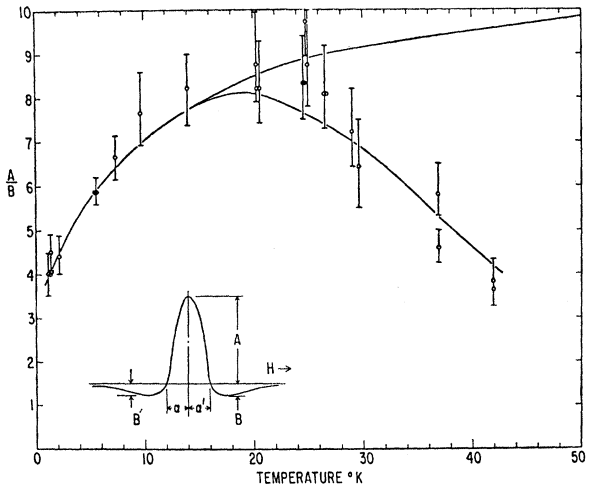

FIG. 5. As shown in the insert, the line shape is characterized by the ratio of the peak (A) to the lobes (B) of the signal amplitudes. This line shape can be predicted knowing the thickness of the sample and the effective spin diffusion length (δ_{eff}). The upper solid line represents a theoretical curve ignoring the effects of phonons. The lower solid line takes into account the effects of both momentum and spin scattering due to the phonons.

agreement and no trace of the A/B "resonance anomaly" reported for Mn in Cu.[11]

(3) *g values.* At higher temperature (~30°K), the g value was close to that for pure copper (g_s), but shifted continuously to lower values as the temperature was lowered. The relative g shift at a given temperature increases with increasing concentration of impurity. These data are shown in Fig. 6.

The procedures by which the values of g_d, T_{sl}, T_{dl}, and χ_r are extracted from the data are as follows:

g_d and χ_r. The susceptibility of the 36-ppm sample was measured on a Faraday balance apparatus as a function of temperature. We find that χ_d may be expressed as $\chi_d = A/T + T'$, with $T' = 1 \pm 0.5$°K. We assume that this temperature dependence of χ_d is the same for all concentrations, and since χ_s is temperature-independent, the temperature dependence of χ_r is known. At a given temperature the value of χ_r will be proportional to the atomic concentration of the local moment. Equation (9) may be rewritten as a linear relation for all concentrations: From the intercept we determine g_d to be 2.006 ± 0.002. Knowing g_d, we can evaluate the coefficient χ_r from the slope. χ_s for the 36-ppm sample could then be determined knowing the experimental value of χ_d. We wish to emphasize that this procedure of measuring χ_s in terms of a known measurement of χ_d circumvents all the problems of determining "effective" impurity concentrations as long as the two experiments are made on the same sample.[31] We find $\chi_s = 1.08 \pm 0.1 \times 10^{-7}$ emu.

[31] More precisely, the only requirement of this method is that in the event of partial oxidation of the impurities, the oxidized species be nonmagnetic; see D. H. Howling, Phys. Rev. **155**, 642 (1967).

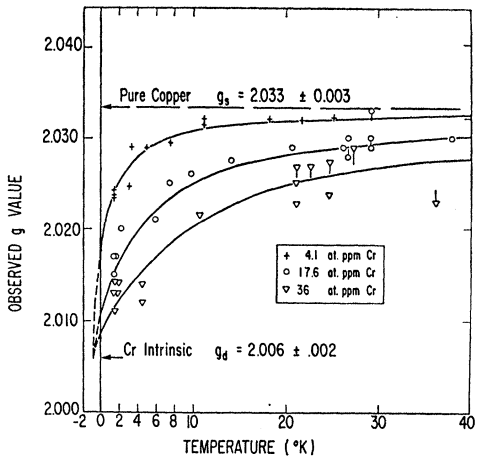

FIG. 6. The g value of the TESR signal as a function of temperature for three different samples. The solid line represents the theoretical predictions for the spin systems [Eq. (9)]. The dotted extrapolation to -1°K corresponds to the fact that the Cr impurities in Cu follow a Curie-Weiss law rather than a Curie law.

T_{sl} and T_{dl}. Equation (11) may be rewritten as

$$\frac{1+\chi_r}{T_{\text{eff}}} = \frac{1}{T_{sl}} + \frac{1}{T_{dl}}\chi_r .$$

Plotting the data in this manner yielded good straight-line fits whose intercepts and slopes yielded values of T_{sl} and T_{dl}, respectively. A plot of T_{sl} versus concentration is shown in Fig. 7. The intercept represents the relaxation rate of the conduction electrons in the starting material and agrees with direct measurements on pure samples. From the slope we determine the spin-flip relaxation rate per ppm to be $1/T_{sl} = 4.8 \times 10^7$ sec^{-1}/ppm at., or, expressed as a spin-flip cross section for electrons scattering on the Cr impurity,

$$\sigma_{\downarrow\uparrow} = 3.6 \pm 0.3 \times 10^{-18} \text{ cm}^2/\text{atom}.$$

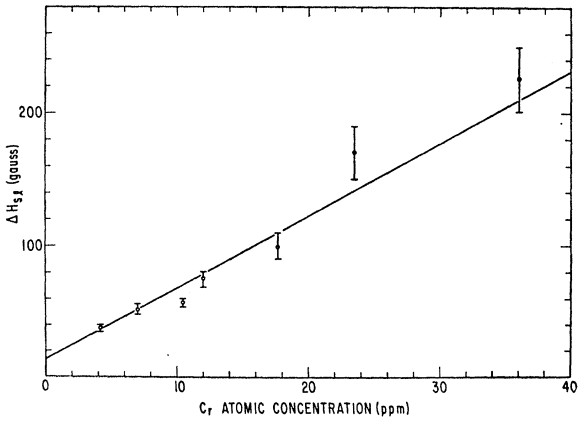

FIG. 7. Spin relaxation rate $1/T_{sl}$ or linewidth ΔH_{sl} of the conduction electrons scattered by Cr impurities as a function of the Cr concentration. From the slope, one can determine the spin-flip cross section per Cr atom. The Cr concentration as measured by atomic absorption and neutron activation agreed within 10%.

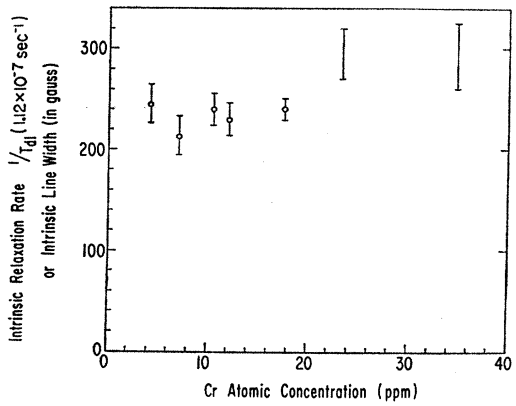

FIG. 8. Intrinsic relaxation rate of Cr in Cu versus Cr concentration. The mechanism providing this intrinsic contribution to the linewidth is as yet unknown. The Cr concentration as measured by atomic absorption and neutron activation agreed within 10%.

In Fig. 8, we present the deduced values of T_{dl} versus concentration. It is seen that there may be a slight concentration dependence, but this is not a major effect. We take

$$1/T_{dl}=2.1\pm0.2\times10^{9}\ \text{sec}^{-1}.$$

V. DISCUSSION

Since we are dealing with the interpretation of the data via a phenomenological model, it is always possible that the identification of the various parameters, like the relaxation rates, are in error or fortuitous. The g-shift formula, Eq. (9), has been derived by utilizing a self-consistent method which lends credence to this feature of the system.[32] Recognizing this inherent reservation about interpreting phenomenological parameters, we wish to comment on the results assuming the model will be fully justified at some future date.

The intrinsic g value for Cr in Cu is, first, very nearly free-electron-like, and, second, very close to the value for Mn in Cu.[11] The main implication would seem to be that the crystal-field splitting effects are suitably small and that the orbital angular momentum is very nearly completely quenched.[33] We know of no theoretical calculations which predict the g values. The susceptibility data yielded a value of the magnetic moment corresponding to a spin of $\frac{3}{2}$. This is a possible value for Cr in an S state (Cr^{+}), which can be shown to be consistent with the very small g shift.[33]

To within the accuracy of the data we found no evidence for a high-temperature g value different from that for the pure copper. This is in contrast to Mn in Cu and Ag, where g deviation plateau effects were reported.[11] As mentioned in Sec. IV, we also found good agreement from the A/B ratio in contrast to the extra peak found in Mn-Cu.[11] We can only conclude that Cr in Cu is a simpler system than Mn in Cu.

We should like to point out that although it is quite clear from the data that a quantity such as T_{dl} is needed, and that while we get a nice self-consistent fit everywhere, assuming it is temperature-independent, we have no explanation at the present for the relaxation mechanism. Certainly any simple process that caused relaxation by interaction with the phonons would have a marked temperature dependence. We know of no calculations which predict values for T_{dl} at the moment.[34]

Since the g-shift relation, Eq. (9), has been derived from a more fundamental view[32] and does not depend on the question of phenomenological relaxation rates, etc., we believe that the extraction of χ_r from the data is on a secure basis. As was discussed in Sec. IV, combining χ_r with the independent measurement of χ_d yields $\chi_s=1.08\pm0.1\times10^{-7}$ emu/g. The quantity χ_s is not expected to be equal to the free-electron value χ_F owing to Fermi-liquid effects. For a metal with a spherical Fermi surface, one could apply the expression for the ratio of the true to the free electron susceptibilities[35]: $\chi_s/\chi_F=(m^*/m)/(1+F_0)$, where m^* is the effective mass as measured from the electronic specific heat and F_0 is the first Legendre coefficient of the spin part of the Landau correlation function. Assuming that this relation is applicable to copper, which has very nearly a spherical Fermi surface, we may determine F_0 by utilizing the measured values of the specific heat[36] via the expression

$$1+F_0=\frac{\gamma_s}{\chi_s}\frac{\chi_F}{\gamma_F}=\frac{\gamma_s}{\chi_s}1.37\times10^{-9},$$

where γ_s and γ_F are the measured and free-electron values for the specific-heat increment/unit temperature, respectively. We find F_0 to be $+0.38\pm0.1$ for copper based on the above analysis. This indicates that the interactions tend to decrease rather than enhance the susceptibility of the electrons.

It is interesting to compare the value of the spin-flip cross section of the Cr impurities with those of other transition metals: Ti, Ni, and Mn.[8,11,37] For these four impurities in copper the cross section lies between 1 and 4×10^{-18} cm^2. This relatively constant value of the cross section indicates that the dominant contribution to the conduction electron relaxation rate is probably due to spin-orbit coupling, and is independent of the

[32] D. R. Fredkin, C. Caroli, and B. Caroli (to be published).
[33] Support to this point of view could be taken from Y. Yafet, Bull. Am. Phys. Soc. **13**, 385 (1968); and Y. Yafet (private communication).
[34] A possible contribution to T_{dl} is discussed by D. C. Langreth, D. L. Cowan, and J. W. Wilkins (unpublished report), but is negligible in our case.
[35] D. Pines and P. Nozières, *The Theory of Quantum Liquids* (W. A. Benjamin, Inc., New York, 1966), Vol. I, p. 197.
[36] D. W. Osborne, H. E. Flotow, and F. Schreiner, Rev. Sci. Instr. **38**, 159 (1967).
[37] We have recently completed a study of the spin-flip cross section for both magnetic and nonmagnetic impurities in copper, which will be discussed in a separate paper.

magnetic properties of the impurities. It should be noted, however, that the values for the intrinsic relaxation rate $(1/T_{dl})$ of the magnetic impurities differ by an order of magnitude for Mn and Cr and by two orders of magnitude for Fe.[38]

VI. CONCLUSION

In conclusion, we summarize briefly the experimental results of this work and their possible theoretical implications: The observation of TESR in dilute Cu-Cr alloys strongly suggests the feasibility of analogous studies on other systems. These include both transition and rare-earth metallic impurities in different metals. From the analysis of the signal behavior as a function of temperature and concentration, a very good fit is made to the phenomenological model of Hasegawa (suitably modified). From this fit the intrinsic g value of Cr, the intrinsic relaxation rate of Cr, and its spin scattering cross section are deduced along with a determination of the spin susceptibility of pure copper. This determination throws some insight on the Fermi-liquid behavior of the electrons of the host metal.

The main questions raised by these results are: Why is the g factor of Cr so near the free-electron value? What is the strong mechanism responsible for the intrinsic relaxation rate $(1/T_{dl})$ of Cr, and why is it temperature-independent? Why is the Kondo scattering phenomena apparently absent from the dynamic behavior of this spin system down to a temperature close to the Kondo temperature?

[38] From Ref. 11; T_{dl} for Mn is 2.9×10^{-9} sec, our value for Cr is 5×10^{-10} sec, and our preliminary value for Fe is $\sim5\times10^{-12}$ sec.

ACKNOWLEDGMENTS

We want to express our thanks to L. Creveling for performing the measurement of the static susceptibilities. We thank Dominique Jérome for neutron-activation analysis of the samples and Professor M. N. A. Peterson for generously helping with our chemical analysis. We are grateful to M. R. Shanabarger and Dr. Y. Yafet for many helpful discussions.

PHYSICAL REVIEW VOLUME 173, NUMBER 3 15 SEPTEMBER 1968

Lattice-Dynamical Properties of Fe^{57} Impurity Atoms in Pt, Pd, and Cu from Precision Measurements of Mössbauer Fractions*

RUDI H. NUSSBAUM, DONALD G. HOWARD, WILBUR L. NEES, AND CHARLES F. STEEN
Portland State College, Portland, Oregon 97207

(Received 25 April 1968; revised manuscript received 6 June 1968)

Precision measurements of the Mössbauer fractions of Fe^{57} in single crystals of Cu, Pd, and Pt were obtained over a range from liquid-helium temperatures to around 750°K in about 50°K intervals, using the "black wide absorber" technique. The over-all accuracy is estimated to be better than 0.7%, with a somewhat larger error for Pt. Our data are consistent with a harmonic lattice with small cubic and quartic anharmonic contributions. Properly weighted Debye temperatures $\Theta_D(-1)$ and $\Theta_D(-2)$ were derived from the low- and high-temperature limits of our f measurements, which were compared with equivalent data for the pure hosts. We conclude that Fe in Cu is about 20% more strongly bound than Cu in Cu, while Fe in Pd and Pt shows about a 20% weaker average force constant than the host atoms. Fe in Cu also has a much larger degree of anharmonicity than pure Cu. Analysis of earlier data on Fe in Ni shows a similar behavior. Our data were also examined for evidence of localized impurity modes. The low-temperature data for Fe in Pt are consistent with the existence of a predicted localized mode, but they do not provide unambiguous evidence.

1. INTRODUCTION

THE probability for the emission of γ rays from radioactive atoms without energy exchange with the lattice vibrations of the crystal in which they are embedded (the Mössbauer effect) depends upon the strength of the interatomic forces between these atoms and the crystal. Precision measurements of the temperature-dependent Mössbauer fraction f (also known as the Debye-Waller factor) yield the temperature dependence of the mean-squared displacement of the emitting nucleus[1] $f(T)=\exp(-\kappa^2\langle x^2\rangle_T)$, where κ is the wave number of the Mössbauer γ ray. In particular, if the Mössbauer atoms are dilute impurities in pure host materials, such measurements may yield rather unique information of the impurity-to-host binding relative to the host-to-host binding, provided that similar lattice dynamical data for the host material are available for comparison.[1] If measurements of the Mössbauer fraction f are obtained over a range from liquid-helium temperatures to temperatures sufficiently high that classical equipartition of the energy can be expected to hold, the data can be interpreted in terms of the high- and low-temperature

* Work supported by a National Science Foundation Research Grant.

[1] A thorough discussion of the analysis of Debye-Waller factors in terms of lattice dynamics of harmonic crystals is given by R. M. Housley and F. Hess, Phys. Rev. 146, 517 (1966). The reader will find earlier references there.